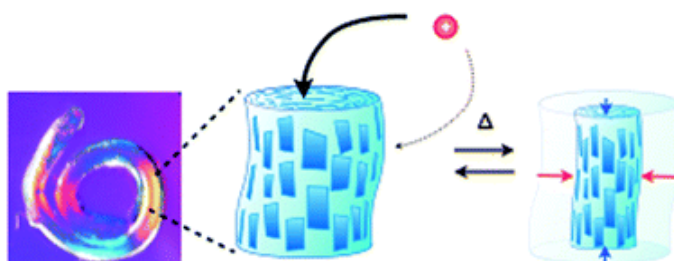


- Liquid crystalline inorganic nanosheets for facile synthesis of polymer hydrogels with anisotropies in structure, optical property, swelling/deswelling, and ion transport/fixation
Miyamoto, N.; Shintate, M.; Ikeda, S.; Hoshida, Y.; Yamauchi, Y.; Motokawa, R.; Annaka, M. *Chem. Commun.* **2013**, 49, 1082-1084.

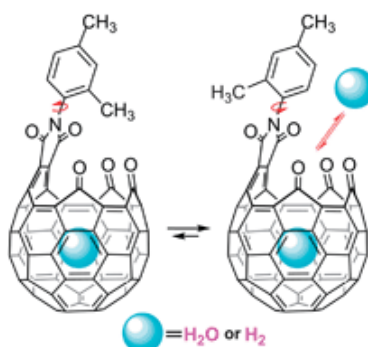
Abstract:



Macroscopically anisotropic hydrogels were synthesized by hybridization of poly(*N*-isopropylacrylamide) with liquid crystalline inorganic nanosheets; their anisotropies in the structure and properties are demonstrated.

- Molecular containers with a dynamic orifice: open-cage fullerenes capable of encapsulating either H₂O or H₂ under mild conditions
Yu, Y.; Shi, L.; Yang, D.; Gan, L. *Chem. Sci.* **2013**, 4, 814-818.

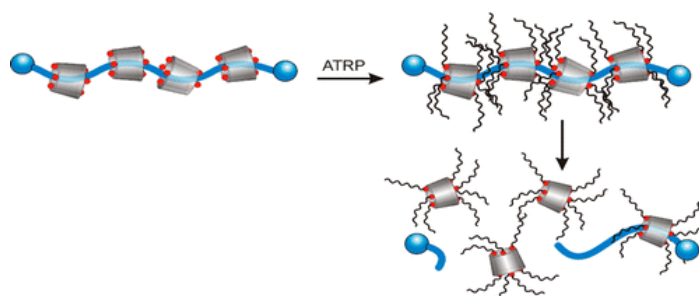
Abstract:



Open-cage fullerene derivatives with an imide moiety above the orifice have been prepared. Rotation of the N-Ar imide bond can tune the orifice to a size large enough to encapsulate H₂O at r.t. and also to a size small enough to keep H₂ from escaping the cavity rapidly.

- Cylindrical Polymer Brushes by Atom Transfer Radical Polymerization from Cyclodextrin-PEG Polyrotaxanes: Synthesis and Mechanical Stability
Teuchert, C.; Michel, C.; Hausen, F.; Park, D.-Y.; Beckham, H. W.; Wenz, G. *Macromolecules* **2013**, 46, 2-7.

Abstract:

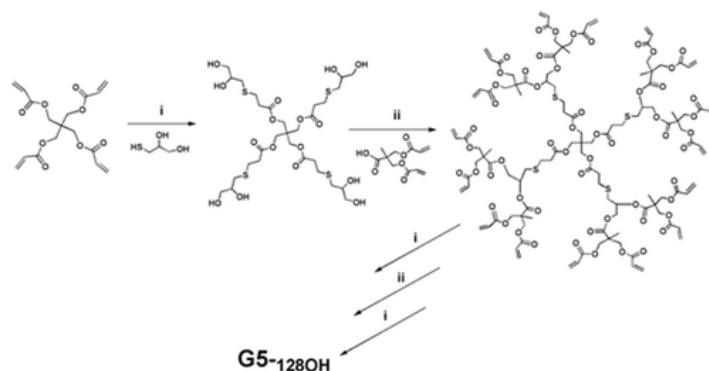


α -Cyclodextrin (α CD) was threaded onto 10 kDa poly(ethylene glycol) (PEG), which was then stoppered with bulky end groups (4-methoxynaphthyl or 9-anthracenylmethyl) to give polyrotaxanes containing about 38 α CD rings threaded onto a PEG backbone. The polyrotaxanes were converted into soluble macroinitiators for atom transfer radical polymerization (ATRP) by esterifying the hydroxyl groups of the threaded α CDs with 2-bromoisobutyryl bromide to a degree of substitution (DS) of 8 per α CD. Living ATRP of methyl methacrylate (MMA) from these polyrotaxane macroinitiators led to polymer brushes with molecular weights of up to 1.7 MDa. Polymer brushes were observed by atomic force microscopy. Surprisingly, large amounts of unthreaded α CD star polymer were observed by GPC. The appearance of these unthreaded α CD star polymers was attributed to the shear-induced rupture of the PEG backbone during passage of the brush through the GPC column. Backbone rupture also occurred upon heating the brushes to elevated temperatures. Proof of the bottle-brush structure was further provided without backbone rupture using diffusion ordered NMR spectroscopy.

- Facile Synthesis of Polyester Dendrimers as Drug Delivery Carriers

Ma, X.; Zhou, Z.; Jin, E.; Sun, Q.; Zhang, B.; Tang, J.; Shen, Y. *Macromolecules* **2013**, *46*, 37-42.

Abstract:

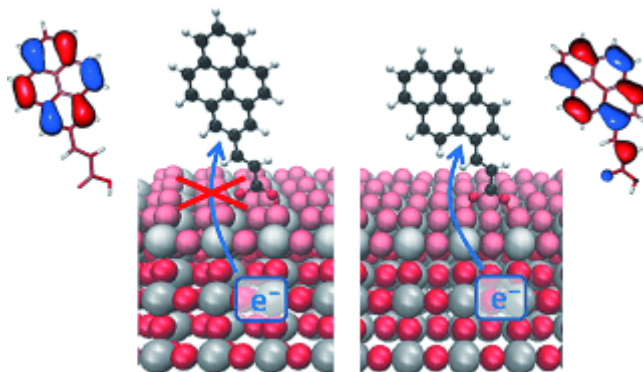


Aliphatic polyester dendrimers are attractive carriers for in vivo delivery of bioactive molecules due to their biocompatibility and biodegradability, but efficient precision synthesis of these dendrimers without tedious purifications remains challenging. Herein, we report an efficient synthesis approach to polyester dendrimers from two AB₂-type monomers via combining a click reaction of thiol/acrylate Michael addition with esterification. The reaction solution of each generation contains only the targeted dendrimer macromolecules; thus, the only required separation is simple precipitation. The resulting hydroxyl-terminated fifth-generation dendrimer is thermoresponsive with a LCST of 41 °C. The dendrimer could be further pegylated to obtain a water-soluble biocompatible dendrimer capable of encapsulation and controlled release of a hydrophobic anticancer drug, doxorubicin.

- Using Orbital Symmetry to Minimize Charge Recombination in DyeSensitized Solar Cells

Maggio, E.; Martsinovich, N.; Troisi, A. *Angew. Chem. Int. Ed.* **2013**, *52*, 973–975.

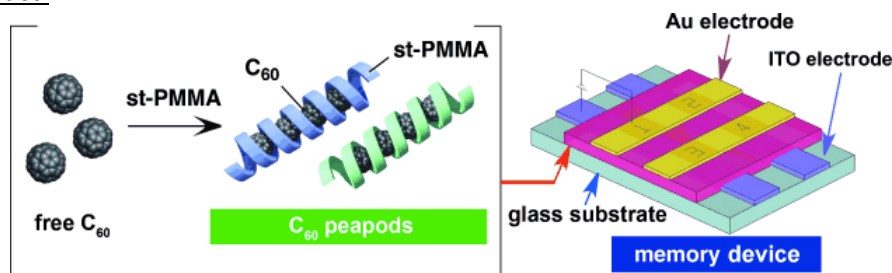
Abstract:



Suitably designed symmetric dyes can be used in dye-sensitized solar cells to reduce the charge recombination rate by two to three orders of magnitude. If the electron coupling between the electrode and the dye is mediated by a conjugated linker, it is possible to design dyes for which the HOMO of the dye is not coupled to the semiconductor.

- Electrical Switching Behavior of a [60]Fullerene-Based Molecular Wire Encapsulated in a Syndiotactic Poly(methyl methacrylate) Helical Cavity
Qi, S.; Iida, H.; Liu, L.; Irle, S.; Hu, W.; Yashima, E. *Angew. Chem. Int. Ed.* **2013**, *52*, 1049–1053.

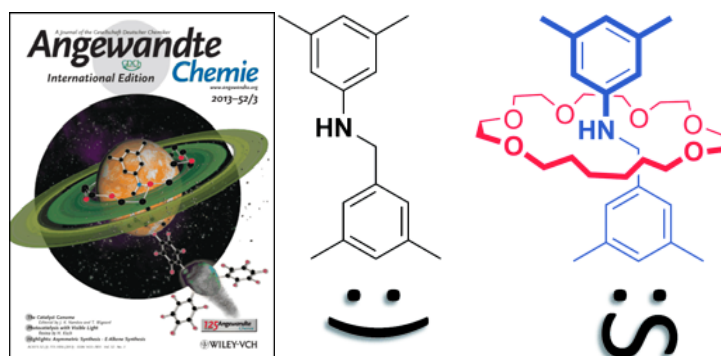
Abstract:



Exploding peapods? A helical syndiotactic poly(methyl methacrylate) encapsulates C_{60} molecules within its helical cavity to form a supramolecular peapod-like molecular wire. Sandwich devices using these molecular wires in the active layer exhibit an irreversible electrical switching effect. Calculations predict a violent Coulomb explosion in the peapod C_{60} wires during the charge injection process, which would account for the observed irreversible electrical switching.

- Heterolytic Activation of H_2 Using a Mechanically Interlocked Molecule as a Frustrated Lewis Base
Caputo, C. B.; Zhu, K.; Vukotic, V. N.; Loeb, S. J.; Stephan, D. W. *Angew. Chem. Int. Ed.* **2013**, *52*, 960–963.

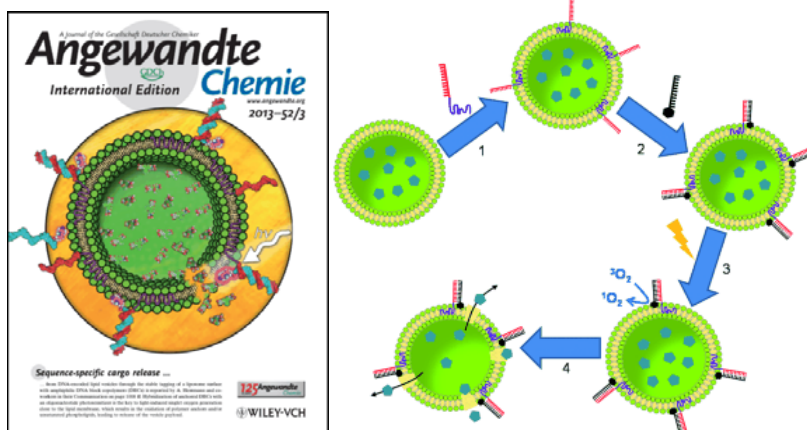
Abstract:



Frustrating: A sterically unencumbered aniline base (see picture, left) can be transformed into a bulky Lewis base by converting it into a [2]rotaxane (right). This Lewis base donor, which is surrounded by a protective macrocyclic ring, exhibits the reactivity of a frustrated Lewis pair (e.g. activation of $H_2(g)$) without the need for direct covalent modification to increase its bulk.

- Light-Triggered Sequence-Specific Cargo Release from DNA Block Copolymer–Lipid Vesicles
Rodríguez-Pulido, A.; Kondrachuk, A. I.; Prusty, D. K.; Gao, J.; Loi, M. A.; Herrmann, A. *Angew. Chem. Int. Ed.* **2013**, *52*, 1008–1012.

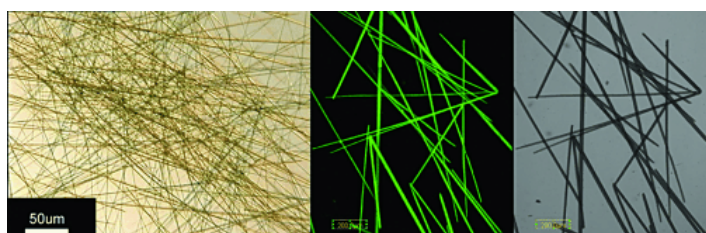
Abstract:



Vesicle buster: Versatile functionalized nanocontainers, based on the stable incorporation of 22 mer DNA-*b*-PPO block copolymers (DBC) into lipid vesicles, are presented (see picture). The study shows effective and sequence-specific cargo release from the DBC–lipid vesicles. Hybridization of these vesicles with an oligonucleotide photosensitizer allows for singlet oxygen generation upon irradiation, which induces cargo release.

- Construction of Supramolecular Self-Assembled Microfibers with Fluorescent Properties through a Modified Ionic Self-Assembly (ISA) Strategy
Zhao, M.; Zhao, Y.; Zheng, L.; Dai, C. *Chem. Eur. J.* **2013**, *19*, 1076–1081.

Abstract:



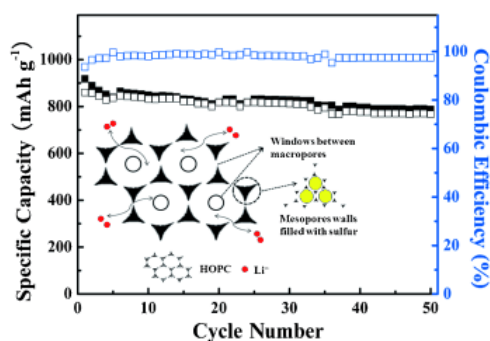
Highly ordered supramolecular microfibers were constructed through a simple ionic self-assembly strategy from complexes of the *N*-tetradecyl-*N*-methylpyrrolidinium bromide ($C_{14}MPB$) surface-active ionic liquid and the small methyl orange (MO) dye molecule, with the aid of patent blue VF sodium salt. By using scanning electron microscopy and polarized optical microscopy, the width of these self-assembled microfibers is observed to be about 1 to 5 μm and their length is from tens of micrometers to almost a millimeter. The 1H NMR spectra of the microfibers indicates that the supramolecular complexes are composed of $C_{14}MPB$ and MO in equal molar ratio. The electrostatic, hydrophobic, and π - π stacking interactions are regarded as the main driving forces for the formation of microfibers. Furthermore, through characterization by using confocal fluorescence microscopy,

the microfibers were observed to show strong fluorescent properties and may find potential applications in many fields.

- Encapsulating Sulfur into Hierarchically Ordered Porous Carbon as a High-Performance Cathode for Lithium–Sulfur Batteries

Ding, B.; Yuan, C.; Shen, L.; Xu, G.; Nie, P.; Zhang, X. *Chem. Eur. J.* **2013**, *19*, 1013–1019.

Abstract:

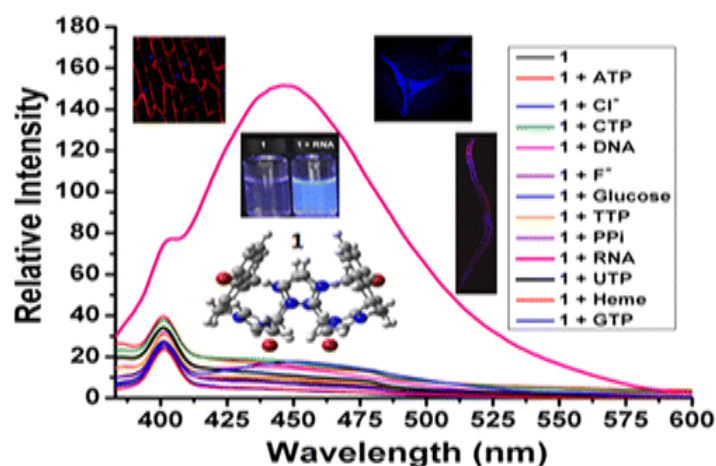


A three-dimensional (3D) hierarchical carbon–sulfur nanocomposite that is useful as a high-performance cathode for rechargeable lithium–sulfur batteries is reported. The 3D hierarchically ordered porous carbon (HOPC) with mesoporous walls and interconnected macropores was prepared by in situ self-assembly of colloidal polymer and silica spheres with sucrose as the carbon source. The obtained porous carbon possesses a large specific surface area and pore volume with narrow mesopore size distribution, and acts as a host and conducting framework to contain highly dispersed elemental sulfur. Electrochemical tests reveal that the HOPC/S nanocomposite with well-defined nanostructure delivers a high initial specific capacity up to 1193 mAh g⁻¹ and a stable capacity of 884 mAh g⁻¹ after 50 cycles at 0.1C. In addition, the HOPC/S nanocomposite exhibits high reversible capacity at high rates. The excellent electrochemical performance is attributed exclusively to the beneficial integration of the mesopores for the electrochemical reaction and macropores for ion transport. The mesoporous walls of the HOPC act as solvent-restricted reactors for the redox reaction of sulfur and aid in suppressing the diffusion of polysulfide species into the electrolyte. The “open” ordered interconnected macropores and windows facilitate transportation of electrolyte and solvated lithium ions during the charge/discharge process. These results show that nanostructured carbon with hierarchical pore distribution could be a promising scaffold for encapsulating sulfur to approach high specific capacity and energy density with long cycling performance.

- Selective Fluorescent Detection of RNA in Living Cells by Using Imidazolium-Based Cyclophane

Shirinfar, B.; Ahmed, N.; Park, Y. S.; Cho, G.-S.; Youn, I. S.; Han, J.-K.; Nam, H. G.; Kim, K. S. *J. Am. Chem. Soc.* **2013**, *135*, 90–93.

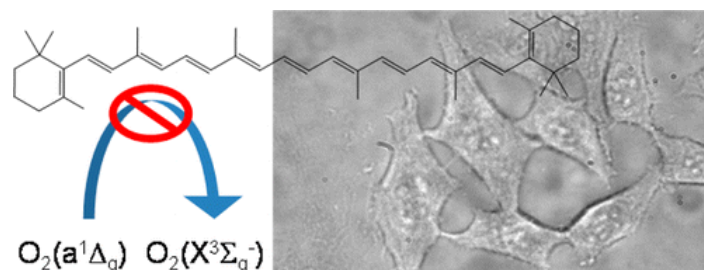
Abstract:



A water-soluble imidazolium-based fluorescent chemosensor senses RNA selectively through fluorescence enhancement over other biologically relevant biomolecules in aqueous solution at physiological pH 7.4. Fluorescence image detection of RNA in living cells such as onion cells, HeLa cells, and animal model cells was successfully demonstrated which displays a chelation-enhanced fluorescence effect. These affinities can be attributed to the strong electrostatic $(C-H)^+ \cdots A^-$ ionic H-bonding and the aromatic moiety driven π -stacking of imidazolium-based cyclophane with the size-complementary major groove of RNA.

- Antioxidant β -Carotene Does Not Quench Singlet Oxygen in Mammalian Cells
Bosio, G. N.; Breitenbach, T.; Parisi, J.; Reigosa, M.; Blaikie, F. H.; Pedersen, B. W.; Silva, E. F. F.; Mártire, D. O.; Ogilby, P. R. *J. Am. Chem. Soc.* **2013**, *135*, 272–279.

Abstract:



Carotenoids, and β -carotene in particular, are important natural antioxidants. Singlet oxygen, the lowest excited state of molecular oxygen, is an intermediate often involved in natural oxidation reactions. The fact that β -carotene efficiently quenches singlet oxygen in solution-phase systems is invariably invoked when explaining the biological antioxidative properties of β -carotene. We recently developed unique microscope-based time-resolved spectroscopic methods that allow us to directly examine singlet oxygen in mammalian cells. We now demonstrate that intracellular singlet oxygen, produced in a photosensitized process, is in fact not efficiently deactivated by β -carotene. This observation requires a re-evaluation of β -carotene's role as an antioxidant in mammalian systems and now underscores the importance of mechanisms by which β -carotene inhibits radical reactions.

- A Chemistry-Based Method To Detect Individual Telomere Length at a Single Chromosome Terminus
Ishizuka, T.; Xu, Y.; Komiyama, M. *J. Am. Chem. Soc.* **2013**, *135*, 14–17.

Abstract:

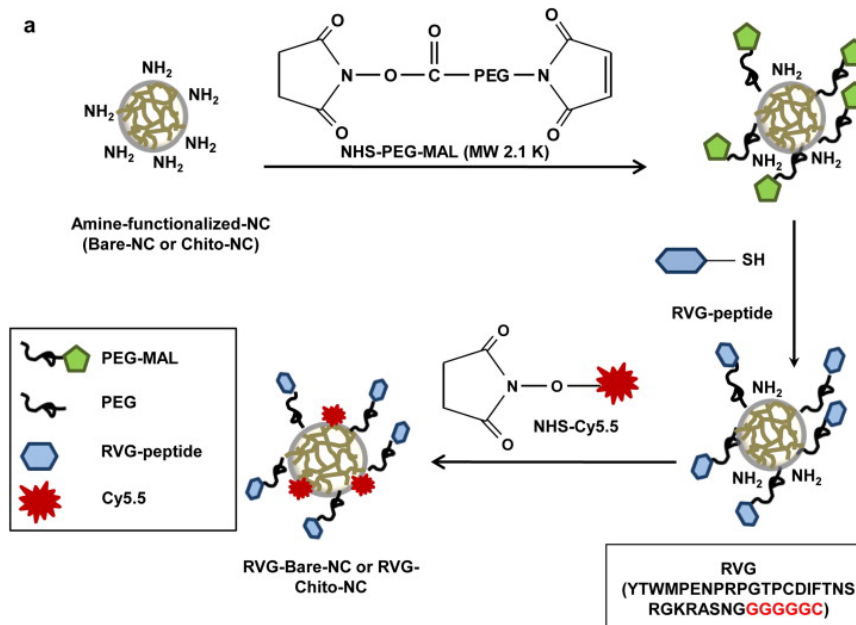


The understanding of telomeres is expected to provide major insights into genome stability, cancer, and telomere-related diseases. In recent years, there have been considerable improvements in the technologies available to determine the length of telomeres of human chromosomes; however, the present methods for measuring telomere length are fraught with shortcomings that have limited their use. Here we describe a method for detection of individual telomere lengths (DITL) that uses a chemistry-based approach that accurately measures the telomere lengths from individual chromosomes. The method was successfully used to determine telomere DNA by breaking in the target sequence and producing a “real telomere fragment.” The DITL approach involves cleavage of the sequence adjacent to the telomere followed by resolution of the telomere length at the nucleotide level of a single chromosome. Comparison of the DITL method and the traditional terminal restriction fragment (TRF) analysis indicates that the DITL approach appears to be promising for the quantification of telomere repeats in each chromosome and the detection of accurate telomere lengths that can be missed using TRF analysis.

- Brain-targeted delivery of protein using chitosan- and RVG peptide-conjugated, pluronic-based nano-carrier

Kim, J.-Y.; Choi, W. I.; Kim, Y. H.; Tae, G. *Biomaterials* **2013**, *34*, 1170-1178.

Abstract:



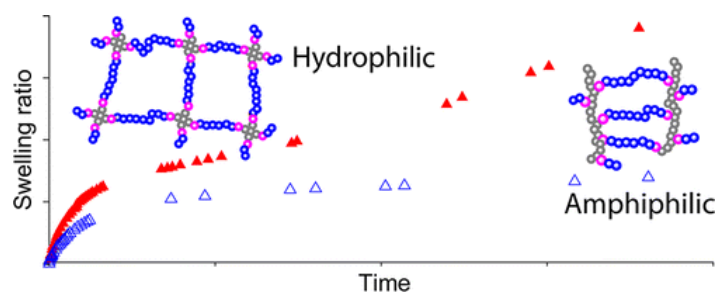
Brain-targeted delivery of drug or imaging agent is hard to achieve efficiently due to the infiltrative nature of the blood-brain barrier (BBB). Moreover, delivery of therapeutic proteins to brain tissue is further limited by the size and physic-chemical properties of proteins. In this work, we developed a chitosan-conjugated Pluronic-based nano-carrier with a specific target peptide for the brain (rabies

virus glycoprotein; RVG29) and applied for the protein delivery to the brain. The *in-vivo* brain accumulation of the nano-carrier in mice followed *i.v* injection was optically monitored with Cy5.5-conjugation to the nano-carrier, and the result showed that the Pluronic-based nano-carrier conjugated with both chitosan and the peptide was very efficient for the accumulation in brain tissue and was remarkably better than the nano-carrier conjugated with the peptide only. β -galactosidase, a model protein, was also delivered and accumulated efficiently in the brain by loading in the nano-carrier, analyzed by the bio-distribution of β -galactosidase. The delivered protein in the brain also maintained its bioactivity. Therefore, RVG29- and chitosan-conjugated Pluronic-based nano-carrier could be potentially useful for the diagnosis and therapy of brain diseases.

- Hydrophilic and Amphiphilic Polyethylene Glycol-Based Hydrogels with Tunable Degradability Prepared by “Click” Chemistry

Truong, V.; Blakey, I.; Whittaker, A. K. *Biomacromolecules* **2012**, *13*, 4012-4021.

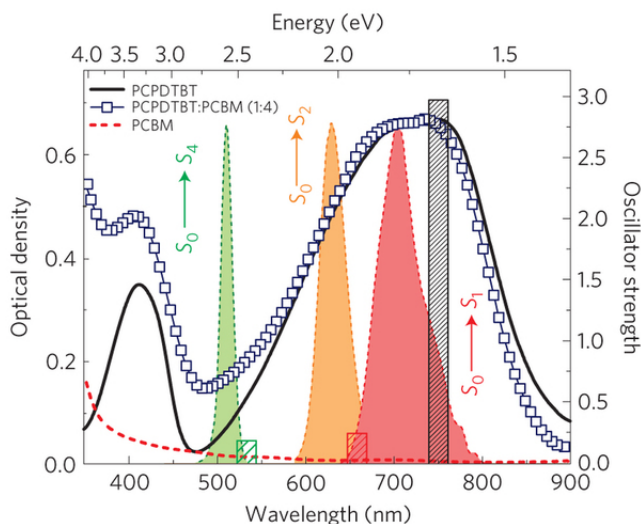
Abstract:



Hydrogels with tunable degradability have potential uses in a range of applications including drug delivery and tissue scaffolds. A series of poly(ethylene glycol) (PEG) hydrogels and amphiphilic PEG-poly(trimethylene carbonate) (PTMC) hydrogels were prepared using copper-catalyzed Huisgen’s 1,3-dipolar cycloaddition, or “click” chemistry as the coupling chemistry. The fidelity of the coupling chemistry was confirmed using Fourier transform infrared (FTIR) and ^1H magic angle spinning (MAS) NMR spectroscopy while thorough swelling and degradation studies of the hydrogels were performed to relate network structure to the physical properties. The cross-linking efficiency calculated using the Flory–Rehner equation varied from 0.90 to 0.99, which indicates that the networks are close to “ideal” at a molecular level. However, at the microscopic level cryogenic scanning electron microscopy (cryo-SEM) indicated that some degree of phase separation was occurring during cross-linking. At 37 °C and pH 7.4, the degradation rate of the hydrogels increased with decreasing cross-link density in the network. Introduction of PTMC as the cross-linker produced an amphiphilic gel with higher cross-link density and a longer degradation time. The degradability of the resultant hydrogels could thus be tuned through control of molecular weight and structure of the precursors.

- Hot exciton dissociation in polymer solar cells
Grancini, G.; Maiuri, M.; Fazzi, D.; Petrozza, A.; Egelhaaf, H.-J.; Brida, D.; Cerullo, G.; Lanzani, G. *Nature Materials* **2013**, *12*, 29–33.

Abstract:

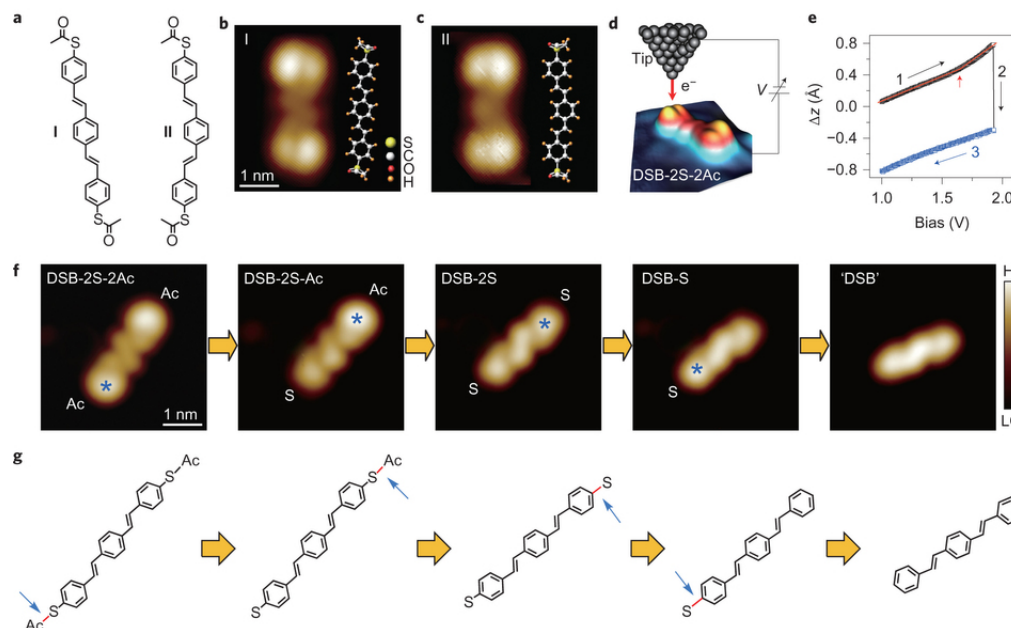


The standard picture of photovoltaic conversion in all-organic bulk heterojunction solar cells predicts that the initial excitation dissociates at the donor/acceptor interface after thermalization. Accordingly, on above-gap excitation, the excess photon energy is quickly lost by internal dissipation. Here we directly target the interfacial physics of an efficient low-bandgap polymer/PC₆₀BM system. Exciton splitting occurs within the first 50 fs, creating both interfacial charge transfer states (CTSs) and polaron species. On high-energy excitation, higher-lying singlet states convert into hot interfacial CTSs that effectively contribute to free-polaron generation. We rationalize these findings in terms of a higher degree of delocalization of the hot CTSs with respect to the relaxed ones, which enhances the probability of charge dissociation in the first 200 fs. Thus, the hot CTS dissociation produces an overall increase in the charge generation yield.

- Submolecular control, spectroscopy and imaging of bond-selective chemistry in single functionalized

Jiang, Y.; Huan, Q.; Fabris, L.; Bazan, G. C.; Ho, W. *Nature Chemistry* **2013**, *5*, 36–41.

Abstract:

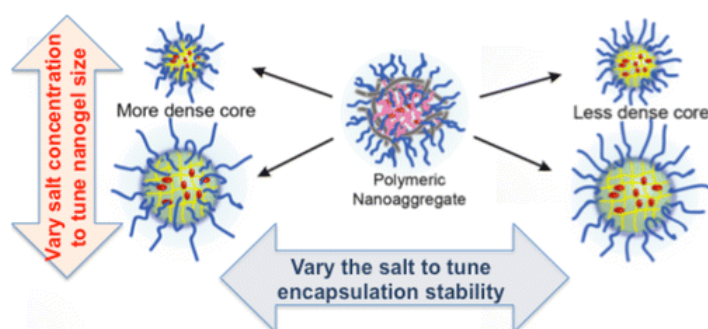


One of the key challenges in chemistry is to break and form bonds selectively in complex organic molecules that possess a range of different functional groups. To do this at the single-molecule level

not only provides an opportunity to create custom nanoscale devices, but offers opportunities for the in-depth study of how the molecular electronic structure changes in individual reactions. Here we use a scanning tunnelling microscope (STM) to induce a sequence of targeted bond dissociation and formation steps in single thiol-based π -conjugated molecules adsorbed on a NiAl(110) surface. Furthermore, the electronic resonances of the resulting species were measured by spatially resolved electronic spectroscopy at each reaction step. Specifically, the STM was used to cleave individual acetyl groups and to form Au–S bonds by manipulating single Au atoms. A detailed understanding of the Au–S bond and its non-local influence is fundamentally important for determining the electron transport in thiol-based molecular junction.

- Effect of Hofmeister Ions on the Size and Encapsulation Stability of Polymer Nanogels
Li, L.; Ryu, J-H.; Thayumanavan, S. *Langmuir* **2013**, *29*, 50–55.

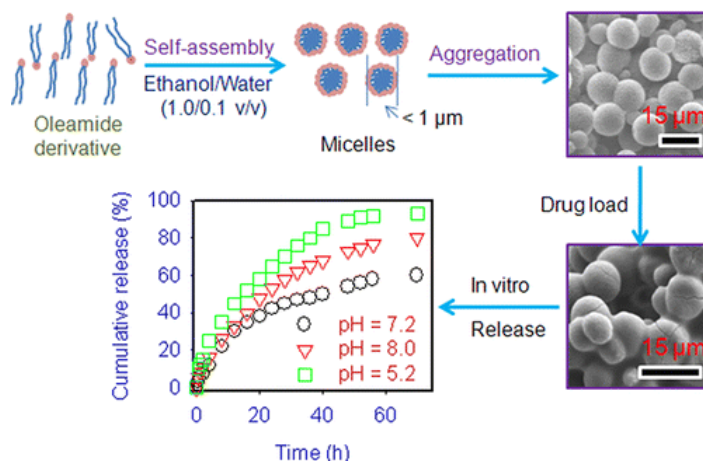
Abstract:



Influence of Hofmeister ions has been investigated on the size and guest encapsulation stability of a polymeric nanogel. While variations in macroscopic phase transitions have been observed in response to the presence of salts, changes in the size and host–guest behavior of polymeric aggregates in the presence of salts have not been explored in any detail. We find that the size and core density of nanogel, which was prepared by self-crosslinking from a random copolymer that contains oligo(ethylene glycol) (OEG) and pyridyl disulfide (PDS) units as side-chain functionalities, can be fine-tuned through the addition of both chaotropes and kosmotropes during nanogel formation. We also demonstrate that the change in core density affects the guest encapsulation stability and stimuli-responsive character of the nanogel.

- Fabrication of Microspheres via Solvent Volatization Induced Aggregation of Self-Assembled Nanomicellar Structures and Their Use as a pH-Dependent Drug Release System
Zhang, L.; Jeong, Y-I.; Zheng, S.; Suh, H.; Hwan Kang, D.; Kim, I. *Langmuir* **2013**, *29*, 65–74.

Abstract:

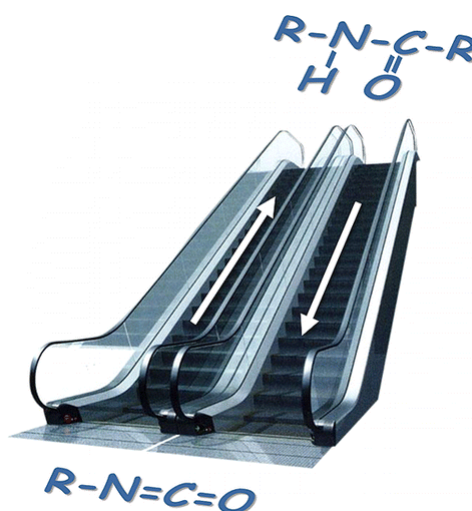


The power conversion efficiency of organic photovoltaic cells depends crucially on the morphology of their donor–acceptor heterostructure. Although tremendous progress has been made to develop new materials that better cover the solar spectrum, this heterostructure is still formed by a primitive spontaneous demixing that is rather sensitive to processing and hence difficult to realize consistently over large areas. Here we report that the desired interpenetrating heterostructure with built-in phase contiguity can be fabricated by acceptor doping into a lightly crosslinked polymer donor network. The resultant nanotemplated network is highly reproducible and resilient to phase coarsening. For the regioregular poly(3-hexylthiophene):phenyl-C61-butyrate methyl ester donor–acceptor model system, we obtained 20% improvement in power conversion efficiency over conventional demixed blend devices. We reached very high internal quantum efficiencies of up to 0.9 electron per photon at zero bias, over an unprecedentedly wide composition space. Detailed analysis of the power conversion, power absorbed and internal quantum efficiency landscapes reveals the separate contributions of optical interference and donor–acceptor morphology effects.

- On the Versatility of Urethane/Urea Bonds: Reversibility, Blocked Isocyanate, and Non-isocyanate Polyurethane

Delebecq, E.; Pascault, J.-P.; Boutevin, B.; Ganachaud, F. *Chem. Rev.* **2013**, *113*, 80–118.

Abstract:



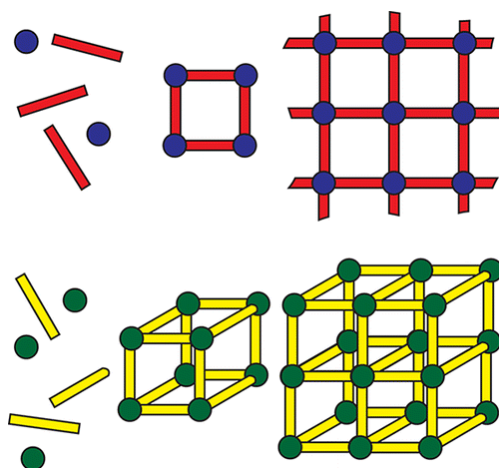
“Discovered by Wurtz in 1848, the isocyanates revealed their chemistry from systematic study during the nineteenth century, for example, by Curtius or Hofmann. The discovery of polyurethanes (PU), via the reaction of a polyester diol with a diisocyanate, by Bayer and his co-workers in 1937, made the diisocyanates one of the major chemicals produced in the world. Currently, the global isocyanate

market grows by 5% per year, stimulated primarily by the polyurethane output expansion. The strength of the polyurethane market surely comes from the fact that a large variety of products can be prepared from essentially simple precursors, namely, toluene diisocyanate (TDI) and methylene diphenyl isocyanate (MDI), used for the manufacture of flexible and rigid polyurethane products, respectively. Depending on whether linear or cross-linked networks are prepared, thermoplastic elastomers and thermoset resins (including foams) are sold every day as major components from paints to binders to materials for the aeronautic industry, for instance. The large range of mechanical properties that can be reached within such materials arise mainly from two physical chemical processes, that is, phase separation between hard and soft segments and hydrogen bonding between carbamate (or urethane) bonds. Another important advantage of isocyanate chemistry is its very deep reactivity and the large yield of reaction one achieves, even in viscous systems or at low temperatures. One major drawback is the inherent toxicity of isocyanate molecules, which in the context of REACh becomes more and more problematic...”

- Metal–Organic Frameworks and Self-Assembled Supramolecular Coordination Complexes: Comparing and Contrasting the Design, Synthesis, and Functionality of Metal–Organic Materials

Cook, T. R.; Zheng, Y.-R.; Stang, P. J. *Chem. Rev.* **2013**, *113*, 734–777.

Abstract:

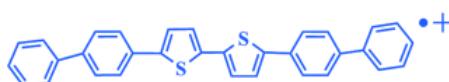
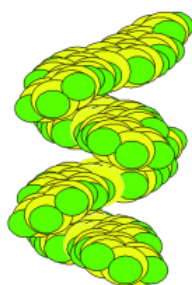


“In 1893, Alfred Werner described the structure of octahedral transition metal complexes and provided the basis for assigning coordination number and oxidation state to what were then known as double salts. This term arose from the observation that transition metal ions appeared to form bonds not only to anionic ligands with which to neutralize their charge, but also to additional species, which seemed unnecessary since neutrality was already achieved. This work was the origin of modern coordination chemistry and greatly expanded the field of inorganic chemistry. By understanding the preferred coordination geometry about a metal ion, rational synthetic methodologies to install specific ligands was now possible. The past 119 years have witnessed a tremendous growth in coordination chemistry, leading to advances in our understanding of the synthesis, structure, and reactivity of novel complexes and materials from simple metal–ligand complexes to organometallic catalysts and extended inorganic polymers. In recent decades, two new branches of coordination chemistry have emerged, metal–organic frameworks (MOFs) and supramolecular coordination complexes (SCCs). The former are comprised of infinite networks of metal centers or inorganic clusters bridged by simple organic linkers through metal–ligand coordination bonds. The latter encompass discrete systems in which carefully selected metal centers

undergo self-assembly with ligands containing multiple binding sites oriented with specific angularity to generate a finite supramolecular complex. On the most basic level, both SCCs and MOFs share the design of metal nodes linked by organic ligands and such constructs can be broadly defined as metal-organic materials (MOMs)."

- Synthesis, Crystal Structure, and Physical Property of Sterically Unprotected Thiophene/Phenylene Co-Oligomer Radical Cations: A Conductive π - π Bonded Supramolecular *meso*-Helix
Chen, X.; Ma, B.; Chen, S.; Li, Y.; Huang, W.; Ma, J.; Wang, X. *J. Chem. Asian. J.* **2013**, *8*, 238–243.

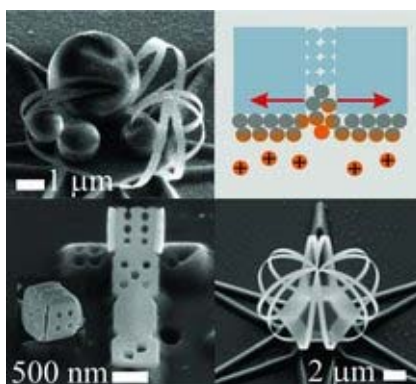
Abstract:



Sterically unprotected thiophene/phenylene co-oligomer radical cation salts $\text{BPnT}^+[\text{Al}(\text{OR}_F)_4]^-$ ($\text{OR}_F = \text{OC}(\text{CF}_3)_3$, $n=1-3$) have been successfully synthesized. These newly synthesized salts have been characterized by UV/Vis-NIR absorption and EPR spectroscopy, and single-crystal X-ray diffraction analysis. Their conductivity increases with chain length. The formed *meso*-helical stacking by cross-overlapping radical cations of BP2T^+ is distinct from previously reported face-to-face overlaps of sterically protected (co-)oligomer radical cations.

- Self-Organized Origami Structures via Ion-Induced Plastic Strain
Chalapat, K.; Chekurov, N.; Jiang, H.; Li, J.; Parviz, B.; Paraoanu, G. S. *Adv. Mater.* **2013**, *25*, 91–95.

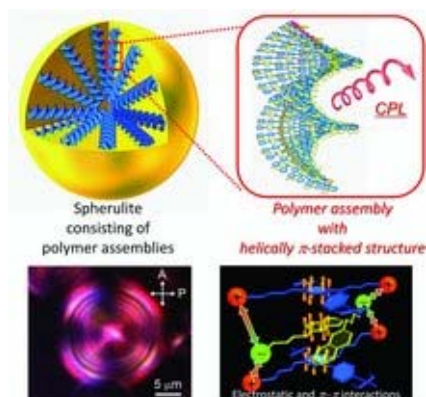
Abstract:



Ion processing of the reactive surface of a free-standing polycrystalline metal film induces a flow of atoms into grain boundaries, resulting in plastic deformation. A thorough experimental and theoretical analysis of this process is presented, along with the demonstration of novel engineering concepts for precisely controlled 3D assembly at micro- and nanoscopic scales.

- Circularly Polarized Blue Luminescent Spherulites Consisting of Hierarchically Assembled Ionic Conjugated Polymers with a Helically π -Stacked Structure
Watanabe, K.; Iida, H.; Akagi, K.; Decorse, P.; Kanoufi, F.; Deronzier, A.; Pinson, J. *Adv. Mater.* **2012**, *24*, 6451–6456.

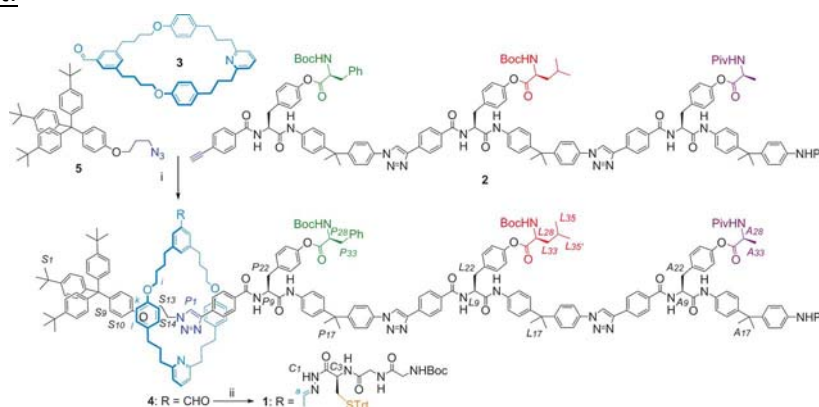
Abstract:



Cationic π -conjugated polymers form an interchain helically π -stacked assembly with anionic chiral compounds that is stabilized by both electrostatic and π - π interactions to hierarchically self-organize into a spherulite with a circularly polarized blue luminescence. To the best of our knowledge, this is the first example of a chiroptical spherulite that is hierarchically constructed from π -conjugated polymers.

- Sequence-Specific Peptide Synthesis by an Artificial Small-Molecule Machine
Lewandowski, B.; De Bo, G.; Ward, J. W.; Pappmeyer, M.; Kuschel, S.; Aldegunde, M. J.; Gramlich, P. M. E.; Heckmann, D.; Goldup, S. M.; D'Souza, D. M.; Fernandes, A. E.; Leigh, D. A. *Science* **2013**, *339*, 189-193.

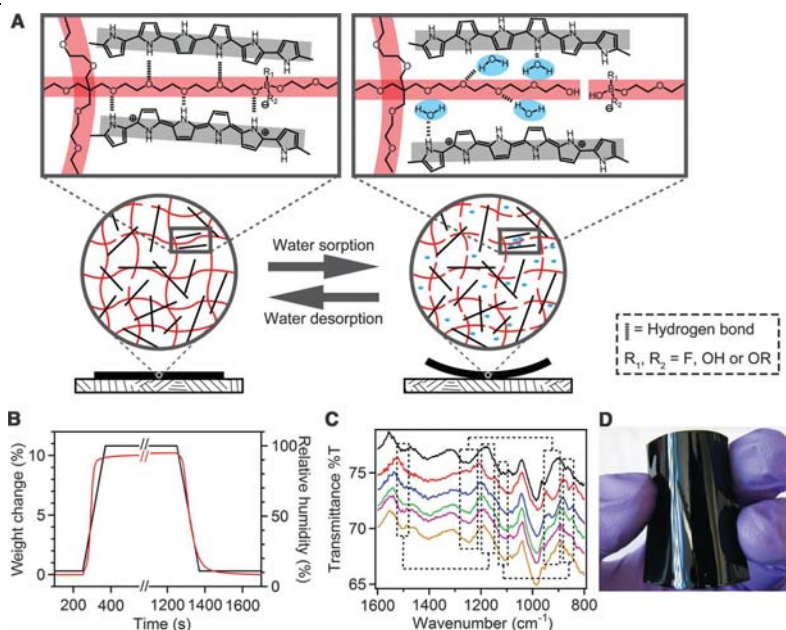
Abstract:



The ribosome builds proteins by joining together amino acids in an order determined by messenger RNA. Here, we report on the design, synthesis, and operation of an artificial small-molecule machine that travels along a molecular strand, picking up amino acids that block its path, to synthesize a peptide in a sequence-specific manner. The chemical structure is based on a rotaxane, a molecular ring threaded onto a molecular axle. The ring carries a thiolate group that iteratively removes amino acids in order from the strand and transfers them to a peptide-elongation site through native chemical ligation. The synthesis is demonstrated with $\sim 10^{18}$ molecular machines acting in parallel; this process generates milligram quantities of a peptide with a single sequence confirmed by tandem mass spectrometry.

- Bio-Inspired Polymer Composite Actuator and Generator Driven by Water Gradient
Ma, M.; Guo, L.; Anderson, D. G.; Langer, R. *Science* **2013**, 339, 186-189.

Abstract:

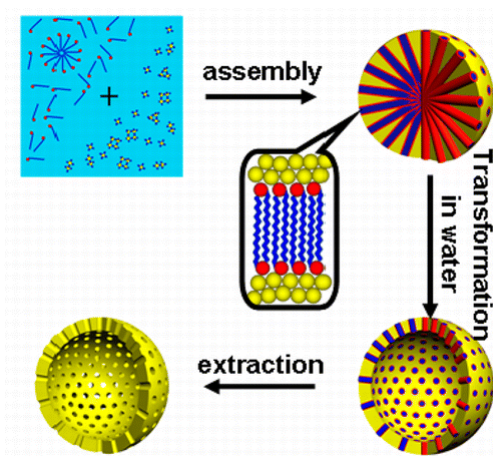


Here we describe the development of a water-responsive polymer film. Combining both a rigid matrix (polypyrrole) and a dynamic network (polyol-borate), strong and flexible polymer films were developed that can exchange water with the environment to induce film expansion and contraction, resulting in rapid and continuous locomotion. The film actuator can generate contractile stress up to 27 megapascals, lift objects 380 times heavier than itself, and transport cargo 10 times heavier than itself. We have assembled a generator by associating this actuator with a piezoelectric element. Driven by water gradients, this generator outputs alternating electricity at ~ 0.3 hertz, with a peak voltage of ~ 1.0 volt. The electrical energy is stored in capacitors that could power micro- and nanoelectronic devices.

- Mesoporous Silica Hollow Spheres with Ordered Radial Mesochannels by a Spontaneous Self-Transformation Approach

Teng, Z.; Su, X.; Zheng, Y.; Sun, J.; Chen, G.; Tian, C.; Wang, J.; Li, H.; Zhao, Y.; Lu, G. *Chem. Mater.* **2013**, 25, 98-105.

Abstract:

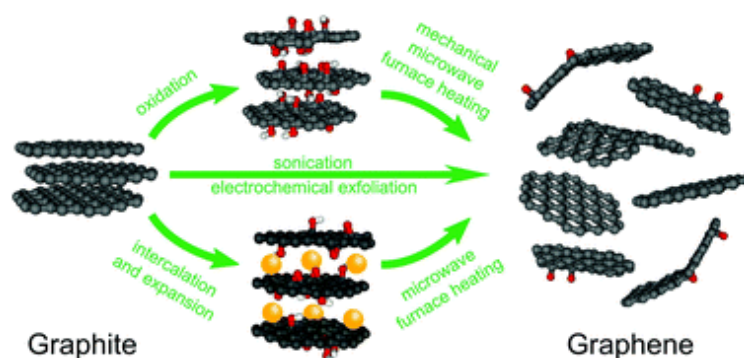


We demonstrate a self-transformation approach for the synthesis of ordered mesoporous silica hollow spheres with radially oriented mesochannels. The method is simple and facile, in which mesostructured silica spheres synthesized in a Stöber solution can spontaneously transform to hollow structure when they are incubated with water. The formation of the hollow structure does not require any sacrificial templates, emulsion droplets, or surface protective agents. The obtained mesoporous silica hollow spheres possess controllable diameter, tunable shell thickness, high specific surface area, and uniform mesopore. Transmission electron microscopy (TEM) observations show that the formation of the hollow spheres undergoes a selective etching process in the inner section. ^{29}Si NMR spectra and detailed reactions demonstrate that the solid-to-hollow transformation of the Stöber silica spheres in water is attributed to the difference in the degree of condensation of silica between their outer layer and inner section. Cytotoxicity and histological assays confirm that the obtained mesoporous silica hollow spheres possess good biocompatibility. Besides, the capability of the hollow spheres as contrast agents for ultrasound imaging is conducted in vitro. Moreover, yolk-shell microspheres with a $\text{Fe}_3\text{O}_4@n\text{SiO}_2$ core and a mesoporous silica shell are successfully prepared based on the facile self-transformation strategy, which provides a general method to create various yolk-shell structured multifunctional composites for different applications.

- Methods of graphite exfoliation

Cai, M.; Thorpe, D.; Adamson, D. H.; Schniepp, H. C. *J. Mater. Chem.* **2012**, *22*, 24992-25002.

Abstract:

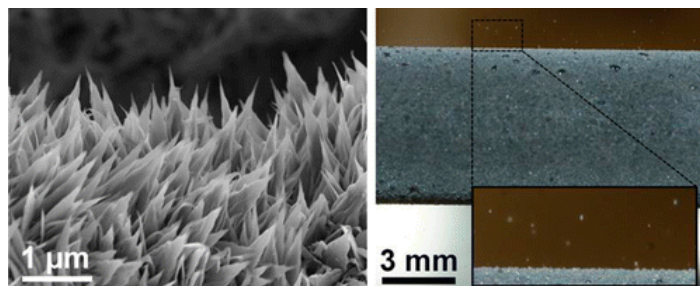


For applications of two-dimensional graphene, commercially viable sources are necessary. Exfoliation from bulk, stacked graphite is the most economical way to achieve large quantities of single layer graphene. A number of methods have been developed to achieve exfoliation of graphite, each with advantages and disadvantages. In this review, we describe current exfoliation methods and techniques used to produce single layer materials from graphite precursors.

- Jumping-Droplet-Enhanced Condensation on Scalable Superhydrophobic Nanostructured Surfaces

Miljkovic, N.; Enright, R.; Nam, Y.; Lopez, K.; Dou, N.; Sack, J.; Wang, E. N. *Nano Lett.* **2013**, *13*, 179-187.

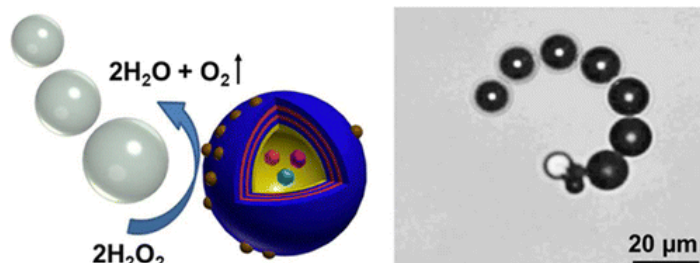
Abstract:



When droplets coalesce on a superhydrophobic nanostructured surface, the resulting droplet can jump from the surface due to the release of excess surface energy. If designed properly, these superhydrophobic nanostructured surfaces can not only allow for easy droplet removal at micrometric length scales during condensation but also promise to enhance heat transfer performance. However, the rationale for the design of an ideal nanostructured surface as well as heat transfer experiments demonstrating the advantage of this jumping behavior are lacking. Here, we show that silanized copper oxide surfaces created via a simple fabrication method can achieve highly efficient jumping-droplet condensation heat transfer. We experimentally demonstrated a 25% higher overall heat flux and 30% higher condensation heat transfer coefficient compared to state-of-the-art hydrophobic condensing surfaces at low supersaturations (<1.12). This work not only shows significant condensation heat transfer enhancement but also promises a low cost and scalable approach to increase efficiency for applications such as atmospheric water harvesting and dehumidification. Furthermore, the results offer insights and an avenue to achieve high flux superhydrophobic condensation.

- Autonomous Movement of Controllable Assembled Janus Capsule Motors
Wu, Y.; Wu, Z.; Lin, X.; He, Q.; Li, J. *ACS Nano* **2012**, 6, 10910-10916.

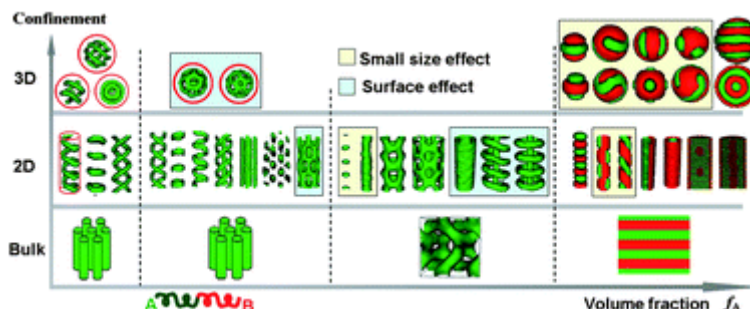
Abstract:



We demonstrate the first example of a self-propelled Janus polyelectrolyte multilayer hollow capsule that can serve as both autonomous motor and smart cargo. This new autonomous Janus capsule motor composed of partially coated dendritic platinum nanoparticles (Pt NPs) was fabricated by using a template-assisted layer-by-layer (LbL) self-assembly combined with a microcontact printing method. The resulting Janus capsule motors still retain outstanding delivery capacities and can respond to external stimuli for controllable encapsulation and triggered release of model drugs. The Pt NPs on the one side of the Janus capsule motors catalytically decompose hydrogen peroxide fuel, generating oxygen bubbles which then recoil the movement of the capsule motors in solution or at an interface. They could autonomously move at a maximum speed of above 1 mm/s (over 125 body lengths/s), while exerting large forces exceeding 75 pN. Also, these asymmetric hollow capsules can be controlled by an external magnetic field to achieve directed movement. This LbL-assembled Janus capsule motor system has potential in making smart self-propelling delivery systems.

- Self-assembly of diblock copolymers under confinement
Shi, A.-C.; Li, B. *Soft Matter* **2013**, *9*, 1398-1413.

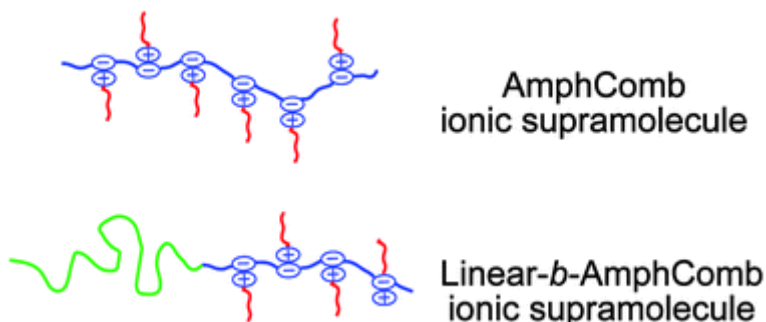
Abstract:



Block copolymers under confinement self-assemble to form various novel structures which are not available in the bulk.

- Micro- and nanophase separations in hierarchical self-assembly of strongly amphiphilic block copolymer-based ionic supramolecules
Ayoubi, M. A.; Zhu, K.; Nystrom, B.; Almdal, K.; Olsson, U.; Piculell, L. *Soft Matter* **2013**, *9*, 1540-1555.

Abstract:



By a selective complexation between different alkyltrimethylammonium amphiphiles (C8, C12 and C16) and three different diblock copolymer systems of poly(styrene)-*b*-poly(methacrylic acid) at various grafting densities X (X = number of alkyl chains per acidic group of the poly(methacrylic acid) PMAA block), a class of ionic supramolecules are successfully synthesized whose molecular architecture consists of a poly(styrene) PS block (Linear block) covalently connected to a strongly amphiphilic comb-like block (AmphComb block), *i.e.* Linear-*b*-AmphComb. In the melt state, these ionic supramolecules can show simultaneous microphase (between Linear and AmphComb blocks) and nanophase (within the AmphComb blocks) separations. This leads to the formation of various structure-in-structure two-scale hierarchical self-assemblies, including S-in-S^{LL}, S-in-S^{BCC}, S-in-C, S-in-L and C-in-L, where S, S^{LL}, S^{BCC}, C and L stand for spherical, spherical in liquid-like state, spherical in body-centered-cubic arrangement, cylindrical and lamellar, respectively. Synchrotron small angle X-ray scattering (SAXS) and crossed polarizers, together with SAXS modelling analysis, were used for a detailed structural study of the samples. The morphology of the microphase separated state was mapped out on 'master' microdomain morphology diagrams as a function of the volume fraction of the AmphComb blocks (Φ_{AmphComb}) and the compositional window of each microdomain morphology was determined. It was observed that, (i) within samples based on the same parent diblock copolymer system, the occurrence of a specific microdomain morphology is only dependent on the value of Φ_{AmphComb} , regardless of the grafting density X and the length of the alkyl side-chains, and (ii)

microdomain morphological boundaries occur at Φ_{AmphComb} values of ~ 0.20 (S^{LL}/C and S^{BCC}/C) and ~ 0.28 (C/L). Finally, the specific influences of the strongly amphiphilic nature of the AmphComb blocks on the observed morphological and hierarchical behaviours of our system are discussed. For reference, stoichiometric strongly amphiphilic comb-like (AmphComb) ionic supramolecules, based on complexation between a homopolymer of PMAA and the various alkyltrimethylammonium amphiphiles, were prepared, which nanophase separated into S (C8) or C (C12 and C16) domains.